NIH Public Access
Author Manuscript
Hepatology. Author manuscript; available in PMC 2013 October 19.

Published in final edited form as:
Hepatology. 2008 July ; 48(1): 289–298. doi:10.1002/hep.22342.

Orphan Receptor Small Heterodimer Partner Suppresses Tumorigenesis by Modulating Cyclin D1 Expression and Cellular Proliferation

Yuxia Zhang[1], **Ping Xu**[1,2], **Kyungtae Park**[3], **Yunhee Choi**[4], **David D. Moore**[5], and **Li Wang**[1]

[1]Departments of Medicine and Oncological Sciences, Huntsman Cancer Institute, University of Utah, Salt Lake City, UT

[2]First Hospital of Sun Yat-Sen University, Guangzhou, China

[3]Department of Microbiology, Molecular Genetics & Immunology, University of Kansas Medical Center, Kansas City, KS

[4]Department of Internal Medicine, University of Texas Southwestern Medical Center, Dallas, TX

[5]Department of Molecular and Cellular Biology, Baylor College of Medicine, Houston, TX

Abstract

The small heterodimer partner (*SHP*; NROB2), a member of the nuclear receptor superfamily, contributes to the biological regulation of several major functions of the liver. However, the role of SHP in cellular proliferation and tumorigenesis has not been investigated before. Here we report that SHP negatively regulates tumorigenesis both *in vivo* and *in vitro*. $SHP^{-/-}$ mice aged 12 to 15 months old developed spontaneous hepatocellular carcinoma, which was found to be strongly associated with enhanced hepatocyte proliferation and increased cyclin D1 expression. In contrast, overexpressing SHP in hepatocytes of *SHP*-transgenic mice reversed this effect. Embryonic fibroblasts lacking *SHP* showed enhanced proliferation and produced increased cyclin D1 messenger RNA and protein, and SHP was shown to be a direct negative regulator of cyclin D1 gene transcription. The immortal $SHP^{-/-}$ fibroblasts displayed characteristics of malignant transformed cells and formed tumors in nude mice.

Conclusion—These results provide first evidence that *SHP* plays tumor suppressor function by negatively regulating cellular growth.

The cell cycle transition from G_0 to S phase is controlled by a series of regulatory events.[1] The cell cycle clock operates by sequential activation and inactivation of several cyclins and cyclin-dependent kinase (CDK) complexes.[2] D-type cyclins bind and activate the Cdk4/6[3] during early to mid G_1, which initiate phosphorylation of the retinoblastoma family of proteins[4,5] and lead to release of the E2F family of transcription factors.[6] E2F triggers expression of genes, including cyclin E and cyclin A, that enables cells to advance into late G_1 and S phases.[7] Activation of cyclin E/Cdk2 complex collaborates with cyclin D/Cdk4–6 for the orderly completion of the G_1-to-S transition.[8,9] The activity of CDKs is negatively regulated by cyclin-dependent kinase inhibitors, including the CIP-KIP family ($p21^{Cip1}$, $p27^{Kip1}$, and $p57^{Kip2}$) and INK family ($p15^{INK4b}$, $p16^{INK4a}$, $p18^{INK4c}$, and $p19^{ARF}$).[10]

Copyright © 2008 by the American Association for the Study of Liver Diseases.

Address reprint requests to: Li Wang, 30 N, 1900 E, SOM 4R118, Salt Lake City, UT84132. l.wang@hsc.utah.edu;fax: 801-587-9415.

Potential conflict of interest: Nothing to report.

Supplementary material for this article can be found on the Hepatology Web site (http://interscience.wiley.com/jpages/0270-9139/suppmat/index.html).

NIH-PA Author Manuscript
NIH-PA Author Manuscript
NIH-PA Author Manuscript

NIH-PA Author Manuscript

NIH-PA Author Manuscript

NIH-PA Author Manuscript

Members of both families of inhibitors are important for executing growth arrest in response to a variety of DNA damage signals.

Genetic aberrations in the regulatory circuits that govern transit through the G_1 phase of the cell cycle occur frequently in human cancers. Perturbation of the cyclin D1/Rb pathway by overexpression of cyclin D1 has been reported as a common alteration leading to a subset of human tumors, including parathyroid adenomas, breast cancer, colon cancer, lymphoma, melanoma, and prostate cancer.[11] Overexpression of cyclin D1 also occurs in human[12] and mouse[13] hepatocellular carcinoma (HCC).

Small heterodimer partner (SHP) is a nuclear receptor functioning as a transcriptional repressor of its target genes.[14] Studies with *SHP* knockouts revealed regulatory functions of SHP in critical aspects of the metabolic disorders.[15–17] In this report, we characterized the novel function of SHP in cellular proliferation associated with HCC formation, using SHP knock-outs, SHP transgenic mice, and mouse embryonic fibroblasts (MEFs).

Materials and Methods

Isolation, Growth, and Immortalization of Fibroblasts

A mutated SHP allele was generated in mice, whereby the exon 1 coding sequence was replaced with a bacterial NLS-LacZ cassette as described.[15] Primary MEFs were isolated from individual E12.5 embryos obtained from crosses between heterozygote $SHP^{+/-}$ animals. The livers of embryos were used for genotyping. All cells were cultured in Dulbecco's modified Eagle's medium (DMEM) containing 10% fetal bovine serum (FBS), in an incubator at 37°C (5% CO_2). Several independently derived immortalized cell lines were generated using a conventional 3T3 protocol that involves passaging cells every 3 days at a fixed cell density.[18] For growth curve experiments, we used the Cell Titer 96 Aqueous One Solution Cell Proliferation Assay (Promega). Proliferating cell nuclear antigen (PCNA) staining (Zymed Laboratories) was performed on liver sections according to the manufacturer's instructions. Protocols for animal use were approved by the Animal Care Committee at the University of Kansas Medical Center.

Fluorescence-Activated Cell Sorting Analysis

Cell cycle parameters were monitored via propidium iodide staining followed by fluorescence-activated cell sorting (FACS) using an Epics XL Flow Cytometer (Coulter). For 5-bromo-2′-deoxyuridine (BrdU)-FACS analysis, cells were incubated with 10 μm of BrdU for 4 hours. Cells were collected, washed, and resuspended in 70% alcohol at 4°C, then stained with anti-BrdU antibody followed by fluorescein isothiocyanate–coupled anti-BrdU secondary antibody (Pharmingen) and prepared for FACS analysis. For cell size analysis, cultures were trypsinized, fixed in 70% alcohol at 4°C, stained with propidium iodide, and analyzed via FACS.

To obtain cells enriched in G1 using hydroxyurea: exponentially growing cells were incubated for 16 hours in complete medium supplemented with 100 mM hydroxyurea (Sigma). To allow cells to progress in the cell cycle, the medium was replaced with DMEM plus 10% FBS and cells were harvested at different times. Synchronization in G_1-S was performed using the double-thymidine procedure: cells were cultured for 8 hours in DMEM plus 10% FBS supplemented with 2 mM thymidine (Sigma), washed twice with phosphate-buffered saline (Invitrogen), cultured for 16 hours in DMEM plus 10% FBS, and finally further incubated for 8 hours in the presence of 2 mM thymidine (Thymidine 0 hours). To allow cells to progress in the cell cycle, the medium was replaced with DMEM plus 10% FBS, and cells were harvested at different times for laser-scanning cytometry. To

NIH-PA Author Manuscript

NIH-PA Author Manuscript

NIH-PA Author Manuscript

synchronize cells at G_2-M phase, cells were incubated with 0.5 μg/mL nocodazole (Sigma) for 16 hours.

Kinase Assay and Immunoblot Analysis

Cyclin D1–associated Rb-kinase assays were performed as follows. Fibroblasts were harvested in ice-cold phosphate-buffered saline and whole cell extracts prepared by sonication in Nonidet P40 lysis buffer containing protein inhibitor cocktail (Amersham) and protein phosphotase inhibitor cocktail (Sigma). Supernatants were then collected, and 50 μg per sample were measured using the Bradford reagent (Sigma). The lysates were incubated for 12 hours at 4°C, with protein A–agarose beads precoated with saturating amounts of the cyclin D1 antibody, DCS-11 (NeoMarkers). Beads containing the immunoprecipitated proteins were washed twice with lysis buffer and twice with kinase buffer, then resuspended in 40 μL of kinase buffer containing substrate (2 μg of soluble GST-RB fusion protein), 10 μM of adenosine triphosphate, and 5 μCi of [γ-^{32}P]adenosine triphosphate (6000 Ci/mmol; Amersham). The samples were incubated for 25 minutes at 30°C with occasional mixing, then boiled in polyacrylamide gel sample buffer containing sodium dodecylsulfate and separated via electrophoresis. Cyclin E–associated H1-kinase assays were performed following the same protocol above, except using cyclin E antibody for immunoprecipitation and histone H1 as the substrate. For immunoblotting analysis, the following antibodies were used: cyclin D2 (Ab-4), cyclin D3 (Ab-1), Cdk2 (Ab-2), Cdk4 (Ab-5), and Cdk6 (Ab-3) from NeoMarkers; cyclin A (C-19), cyclin D1(Ab-2), and cyclin E (M-20) from Santa Cruz Biotechnology; and β-actin from Sigma. Blots were incubated with horseradish peroxidase–conjugated secondary antibodies (Amersham) followed by detection with an electrochemiluminescence detection kit (Pierce).

Adenovirus, RNA Interference Infection, and Northern Blotting

Viruses were generated by Dr. Kazuhiro Oka (Baylor College of Medicine). Cells were plated at 2×10^6 per 10-cm dish and infected the next day with viral supernatant (multiplicity of infection = 50) for 1 hour. SHP small interfering RNA (Ambion) was then transfected into cells. Gene expression was analyzed via northern blotting.[17]

Colony Formation, Tumorigenicity, and Chromosome Analyses

To test for the ability of the cells to form colonies when plated at low density, 1.3×10^3 cells were plated in two 10-cm dishes and were fed every 3 days. Following 2 weeks of culture, dishes were stained with Giemsa, and the number of visible colonies were counted. For tumorigenicity assays, exponentially growing MEF cells (2×10^6) were subcutaneously injected into the scapular region of 6-week-old anesthetized nude mice (Swiss nu/nu; Harlan) with two injection sites per mouse, and tumor development was monitored for 4 to 10 weeks. For chromosome analysis, MEFs were exposed to colce-mid (0.02 μg/mL) for 2 hours. Mitotic chromosome spreads were prepared via standard procedures and stained with 4′,6′-diamidino-2-phenylindole. At least 300 metaphase spreads were analyzed.

Transient Transfection, Mutagenesis, Electrophoretic Mobility-Shift Assay, and Chromatin Immunoprecipitation Assay

Mouse SHP and LRH-1 complementary DNA and mouse cyclin D1 promoter-Luc reporters were obtained from Drs. Yoon Kwang Lee and David Moore. CV1 cells were transfected via the calcium phosphate method. Forty hours after transfection, cell extracts were analyzed for luciferase activity and β-galactosidase (β-gal) activity with a Dual-Luciferase Reporter System (Promega). Transfection efficiency was standardized with β-gal activity. Transfection experiments were performed three times with similar efficiency.

NIH-PA Author Manuscript

NIH-PA Author Manuscript

NIH-PA Author Manuscript

The Exsite polymerase chain reaction–based, site-directed mutagenesis (Stratagene) kit was used to introduce mutation in the LRH-1 binding sites of the −970 mCD1 promoter. Three mutant mCD1-Luc constructs were generated, and correct mutations were confirmed on sequencing. The following primers were used: mut-L1-F, 5′-cgatttgcatatctacgacttctgaggggggaaggggtttg, and mut-L1-R, 5′-caaacccttcccccctcagaagtcgtagatatgcaaatcg; mut-L2-F, 5′-cccctttctctgcccggaagtgatctctgctt aacaac, and mut-L2-R, 5′-gttgttaagcagagatcacttccgggcagagaaaagggg.

The *in vitro*–translated LRH-1 proteins were prepared using a coupled transcription and translation kit (Promega). For protein-DNA interaction, *in vitro*–translated LRH-1 was incubated with the following ^{32}P-labeled duplex oligonucleotide probe: L1-F, 5′-atatctaccaaggct-gagggg, and L1-R, 5′-ccccctcagccttggtagatat; L2-F, 5′-ctgcccggctttgatctctg, and L2-R, 5′-cagagatcaaagccgggcag. Mutant probe L1-mut-F: 5′-atatctaccacttctgagggg and L1-mut-R 5′-ccccctcagaagtggtagatat was used as a competitor. The wild-type and mutant LRH-1 binding sequences are underlined.

Mouse fibroblasts were used and chromatin was cross-linked immunoprecipitated using standard procedures. Immunoprecipitation was performed with 10 μg anti-SHP (Santa Cruz Biotechnology) antibody overnight at 4°C. The primers mD1 SP-F, 5′-cctccacaggtctcggagga, and SP-R, 5′-gccgacagccctctggaggct, were used to amplify the mCD1 fragment including both LRH-1 binding sites (L1 and L2). The primers mD1 NS-F, 5′-accctcaacgaagc-caatca, and NS-R, 5′-tatccccctcctccactgca, were located upstream of the LRH-1 binding sites in mCD1 and were used for nonspecific amplification.

Statistical Analysis

Data are expressed as the mean ± standard deviation. Statistical analyses were performed using the Student unpaired *t* test. $P < 0.05$ was considered statistically significant.

Results

Spontaneous HCC Formation in *SHP*$^{-/-}$ Mice Associated with Massive Hepatocyte Proliferation

The *SHP*$^{-/-}$ mice showed no apparent phenotypic abnormalities of the liver in animals up to 6 months of age.[17] However, by 15 months of age, we observed spontaneous liver tumors in 19 of 35 (55%) *SHP*$^{-/-}$ mice that were examined. The tumors were developed at different stages and histologically spanned the range from microadenomas (Fig. 1A, panel a) to adenocarcinomas (Fig. 1A, panels b and b') to carcinomas (Fig. 1A, panels c and c'). None of the wild-type mice of the same age, maintained under the same conditions, had tumors (panel d). The data suggest that the liver tumors developed in *SHP*$^{-/-}$ mice were due to the long-term effect of loss of *SHP* function.

To determine if changes in hepatocyte proliferation were involved in HCC formation in *SHP*$^{-/-}$ mice, we examined cyclin D1 messenger RNA (mRNA) via northern blotting. The expression of cyclin D1 was up-regulated in *SHP*$^{-/-}$ mice at 12 months of age, and this was pronounced in 15-month old mice (Fig. 1B). However, no changes in cyclin D1 mRNA were seen in the livers of wild-type mice. PCNA staining of liver sections revealed massive hepatic proliferation in *SHP*$^{-/-}$ mice, which was completely reversed by overexpressing SHP in hepatocyte-specific *SHP*-transgenic mice (Fig. 1C and Supplementary Fig. 1A–D). The data suggest that up-regulation of cyclin D1 and enhanced hepatocyte proliferation may contribute to liver tumor formation in *SHP*$^{-/-}$ mice. In addition, SHP expression was barely detectable in mouse hepatoma cell line Hepa-1 cells compared with the normal mouse hepatocyte cell line NMuli (Supplementary Fig. 1E), consistent with the notion that *SHP* deficiency is associated with liver tumor formation in mice. To determine if SHP directly

NIH-PA Author Manuscript

NIH-PA Author Manuscript

NIH-PA Author Manuscript

represses cyclin D1 expression in hepatocytes, we overexpressed SHP back into Hepa-1 cells by SHP adenovirus transduction. Overexpression of SHP decreased cyclin D1 (≈50%) as well as PCNA (≈60%) expression (Fig. 1D and Supplementary Fig. 1F). The data further suggest that cyclin D1 may be a novel SHP target gene.

Enhanced Proliferation of Fibroblasts Lacking *SHP*

MEFs are a well-established *in vitro* model to study cell cycle regulation. To explore the role of SHP in cell cycle progression, MEFs were isolated from E12.5 embryos of heterozygous intercross of $SHP^{+/-}$. Cultures of $SHP^{-/-}$ MEFs were morphologically indistinguishable from those of $SHP^{+/+}$ MEFs. To further understand the growth properties of MEFs, we derived immortalized cells using the conventional 3T3 protocol[18] and observed increased cell proliferation in $SHP^{-/-}$ cells. Compared with wild-type cells, the mutant *SHP* cells were with a spindlelike morphology (Supplementary Fig. 2A) that were approximately 30% smaller than control cells in volume (Supplementary Fig. 2B). The exponential *SHP* mutants showed decreased cells accumulated in G_0/G_1 but increased population of cells in G_2/M phase than wild-type cells (Supplementary Fig. 2C, left). Approximately 14% of > 4n cells was seen in *SHP* mutants, which was detected by BrdU–fluorescein isothiocyanate–FACS analysis (Supplementary Fig. 2C, right). To better understand the role of SHP in cellular progression, the cells were quiescent at G0/G1 by hydroxyurea. The $SHP^{-/-}$ cells maintained a persistent higher S phase cell population than the $SHP^{+/+}$ cells (Fig. 2A and Supplementary Table 1). When cells were synchronized to the G_1/S boundary by double thymidine block procedure, *SHP*-deletion resulted in a higher accumulation of S phase cells and a faster progression into the G_2/M phase (Fig. 2B). When the cells were arrested at G_2/M phase by nocodazole and released into the cell cycle, the $SHP^{-/-}$ cells progressed into G0/G1 phase in a fashion similar to that of $SHP^{+/+}$ cells (Fig. 2C). Thus the $SHP^{-/-}$ cells displayed a higher G_1/S transition capacity than wild-type controls.

To determine the kinetics of cell cycle proliferation, cells were made quiescent by serum deprivation and the cell cycle re-entry was elicited by the addition of fresh serum. The $SHP^{-/-}$ cells exhibited faster growth than wild-type controls (Fig. 2D, left). Overexpression of SHP adenovirus into the null cells decreased the growth rate (Fig. 2D, middle), whereas knocking down SHP of wild-type cells by RNA interference enhanced the proliferation (Fig. 2D, right). The data demonstrated that SHP directly inhibits cell proliferation.

Alterations of Kinase Activities and Cyclins of Fibroblasts Lacking *SHP*

Cell cycle entry of quiescent cells begins with a rapid activation of immediate-early genes,[19] such as the MAPK pathway and the induction of c-fos gene expression. The kinetics of MAPK activation was indistinguishable in $SHP^{+/+}$ and $SHP^{-/-}$ cells (Supplementary Fig. 3A). However, there was a moderate reduction of c-fos (Supplementary Fig. 3B), c-jun, and junB (Supplementary Fig. 3C) expression in $SHP^{-/-}$ cells, indicating a partial impairment in this signal transduction pathway.

As an initial measure of potential cell cycle defect, we determined the kinase activities of cyclin-CDK complexes. A modest increase in cyclin D1–associated kinase activity was observed in $SHP^{-/-}$ cells (Fig. 3A). The largest defect was seen in cyclin E–associated activity, which was defective in $SHP^{-/-}$ cells.

To investigate possible causes of the changed CDK activity, the expression levels of cyclins and CDKs in MEFs were examined via immunoblotting. The D-type cyclins are the first cyclins to be induced during the G_0-to-S transition, followed by cyclin E in late G_1 phase, cyclin A in S phase, and cyclin B in late S and G_2 phase.[2] Cyclin D1 expression was

NIH-PA Author Manuscript

NIH-PA Author Manuscript

NIH-PA Author Manuscript

markedly increased in *SHP*$^{-/-}$ cells (Fig. 3B). There was a reduction in cyclin D2, cyclin E, and Cdk2 expression in *SHP*$^{-/-}$ cells, but no difference in expression of cyclin D3, cyclin A, Cdk4, or Cdk6 in *SHP*$^{+/+}$ and *SHP*$^{-/-}$ cells. Thus, the increased cyclin D1 kinase activity may be responsible for the enhanced proliferation property in *SHP*$^{-/-}$ cells.

SHP Repression of Cyclin D1 mRNA of Embryonic Fibroblasts

To determine if changes in cyclin D1 protein are due to changes in cyclin D1 gene transcription, northern blotting was used to determine cyclin D1 mRNA expression. Cells were starved for 3 days and released into cell cycle, and an elevated level of cyclin D1 mRNA was observed in *SHP*$^{-/-}$ cells, especially at early time points (Fig. 3C, top). Cyclin D1 mRNA was also increased in exponentially growing *SHP*$^{-/-}$ cells (Fig. 3C, bottom, left). In addition, re-expression of SHP in *SHP*$^{-/-}$ cells by adenovirus transduction repressed cyclin D1 mRNA (middle), whereas knocking down SHP expression in wild-type cells by RNA interference effectively increased cyclin D1 mRNA (right). Furthermore, the basal cyclin D1 promoter activity in *SHP*$^{-/-}$ cells was significantly higher than in wild-type cells, and that addition of SHP by adenovirus transduction or coexpression with SHP vector dramatically decreased cyclin D1 activity (Fig. 3D). The data suggest that SHP may directly repress cyclin D1 expression.

SHP Repression of Cyclin D1 Promoter Transactivation

To explore the molecular basis for the inhibition of cyclin D1 expression by SHP, we localized two potential matches to LRH-1 consensus sites on the proximal mouse cyclin D1 (mCD1) promoter between nt −123 to −115 and −242 to −234. Transient transfection with different deletion constructs showed that mCD1 −336, −675 and −970 reporters (containing L1 and L2) were strongly transcribed in response to LRH-1, which was not observed with the −52mCD1 (containing no LRH-1 site) (Supplementary Fig. 4A). The functionality of the proximal −123 to −115 site of mCD1 promoter was confirmed by the dose-dependent transactivation of −187mCD1 (containing one LRH-1 site) by LRH-1 and a dose-dependent repression by SHP (Fig. 4A, left). β-Catenin has been shown to activate human cyclin D1 promoter through the TCF transcription factor,[20] thus we tested the effect of β-catenin, LRH-1, and SHP on mCD1 transactivation using the −970mCD1 (Fig. 4A, right). β-Catenin alone was unable to activate −970mCD1 gene transcription (lane 2 versus 1; Supplementary Fig. 4B). Cotransfection of LRH-1 with β-catenin strongly activated mCD1 (lane 3), and SHP dose-dependently repressed this activation (lanes 4–6). However, the effect on mCD1 gene transcription by β-catenin and LRH-1 (lane 3) did not differ from that of LRH-1 alone (lane 7), suggesting that the effect seen with cotransfection of β-catenin plus LRH-1 was mediated by LRH-1. In addition, with the same amount of SHP, the inhibitory effect of SHP on LRH-1 in the presence of β-catenin (lane 5) was more potent than in the absence of β-catenin (lane 8). Moreover, in the absence of LRH-1, cotransfection of SHP with β-catenin showed a modest inhibitory effect on mCD1 activity that was below the basal level. Cotransfection with β-catenin had no effect or mildly inhibitory effects on LRH-1 activation of the mouse SHP promoter (Supplementary Fig. 4C).

The function of the two LRH-1 binding sites (L1 and L2) was confirmed using mutagenesis (Fig. 4B). Interestingly, disruption of L1 resulted in a 90% decrease in mCD1 gene transcription, whereas mut2 lost approxi-mately 60% of the transactivation produced by LRH-1. Unexpectedly, the double mutant (mut3) did not completely abolish LRH-1–mediated transcription. It is possible that additional nonconsensus but weak LRH-1 sites might exist within the −970mCD1 promoter region. The binding activities of the L1 and L2 sequences were analyzed via electrophoretic mobility-shift assay using the oligonucleotides listed in Materials and Methods. When the oligonucleotides containing L1 and L2 were incubated with an *in vitro* synthesized LRH-1, both L1 and L2 competed for LRH-1 binding,

NIH-PA Author Manuscript

NIH-PA Author Manuscript

NIH-PA Author Manuscript

whereas mutant L1 had no effect (Fig. 4C). Chromatin immunoprecipitation assays confirmed the coimmunoprecipitation of SHP with mCD1 in MEFs (Fig. 4D). Because LRH-1 is expressed in MEFs (Supplementary Fig. 5A), these studies demonstrate that SHP is a transcriptional repressor of cyclin D1 gene transcription by LRH-1.

Malignant Transformation of Immortal Fibroblasts Lacking SHP

Although the *SHP*$^{-/-}$ cells were smaller, they reached higher density at confluence, lost contact inhibition property, and failed to undergo cell cycle arrest, all of which are hallmarks of transformed cells. To investigate the tumorigenicity of *SHP*$^{-/-}$ cells, we analyzed malignant features of the cells. *SHP*$^{-/-}$ cells exhibited increased colonies in soft agar (Fig. 5A) and tumor formation in nude mice (Fig. 5B). In contrast, matched control wild-type cells showed fewer colonies and did not form tumors within 6 weeks when the experiment was conducted. We ask if genetic alterations occurred in the immortal *SHP*$^{-/-}$ cells, and if *SHP* deficiency could contribute to such alterations. In support of this hypothesis, *SHP*$^{-/-}$ MEFs displayed an increased number of aberrations, such as many short chromosomes, which were rarely observed in *SHP*$^{+/+}$ cells (Fig. 5C). To determine if decreased cyclin D1 expression is associated with the tumorgenic property of the cells, we overexpressed SHP using adenovirus into *SHP*$^{-/-}$ cells and examined its effect on foci formation. As expected, over-expression of SHP repressed cyclin D1 expression (Supplementary Fig. 5B) and reduced the number of foci formation (Fig. 5D). The data suggest that loss of SHP resulted in aberrant cell proliferation and cyclin D1 expression, which is associated with the transformed phenotype.

Discussion

The effects of orphan nuclear receptor SHP on cellular proliferation and transformation have not been documented before. In this study, we show that deletion of *SHP* results in enhanced hepatocyte proliferation, which is directly associated with the development of liver tumor. We further show that the impaired function of *SHP* causes perturbations in growth of *SHP*$^{-/-}$ MEF cells. SHP regulates cell proliferation through repression of cyclin D1, thereby providing a novel molecular link between SHP and the cell cycle machinery. Deletion of *SHP* in fibroblasts causes a phenotype characterized by transformation of immortalized MEFs. Our results reveal a unique role for SHP in mediating cell growth associated with the development of HCC.

Despite extensive studies of tumor suppressor genes, there are presently no excellent mouse models demonstrating increased susceptibility to liver tumors.[21] Suggested mechanisms of liver tumor formation are enhanced cell replication, promotion of spontaneous preneoplastic lesions, and inhibition of apoptosis. Abnormal expression of cyclin D1 has been described in liver cancers in both mice[13] and humans.[12] Our data provide new evidence that the enhancement of cyclin D1 expression and hepatocyte proliferation contribute to the development of liver cancer in *SHP*$^{-/-}$ mice. Thus, SHP may play a tumor suppressor function in the development of HCC.

SHP$^{-/-}$ mice did not show overt growth defects after birth,[17] thus SHP is apparently dispensable for normal mouse embryogenesis. However, examination of *SHP*$^{-/-}$ fibroblasts indicates that SHP is required during continuous proliferation. Our analysis indicates that impaired function of *SHP* causes enhanced growth of *SHP*$^{-/-}$ fibroblasts. The increases in the expression levels of cyclin D1, cyclin D1 kinase activity, and subsequently the activation of E2F (Supplementary Fig. 5C), matches well with that in the increased cell proliferation in *SHP*$^{-/-}$ MEFs. For correct regulation of CDK activities, the amount of G1 cyclins, as well as CDK and cyclin-dependent kinase inhibitors will be tightly regulated within a certain range. The hyperproliferation occurs despite inactivation of cyclin E kinase activity, suggesting

NIH-PA Author Manuscript

NIH-PA Author Manuscript

NIH-PA Author Manuscript

that cyclin E and Cdk2 are nonessential mediators for SHP-induced antiproliferative signaling. Because cyclin D1 and cyclin E subserve at least partially overlapping functions, and the roles of cyclin E and Cdk2 are dispensable in controlling cell cycle progression,[22,23] the increased cyclin D1–associated kinase activity in *SHP*$^{-/-}$ cells may play a major role for the increased cell proliferation property.

A recent report describes the role of LRH-1 in enhancing cell proliferation through targeting cyclin D1 and cyclin E.[24] In general, our results are similar and support the conclusion of a negative regulatory role of SHP on cyclin D1 transcription.[24] However, we observed decreased cyclin E and Cdk 2 protein levels in *SHP*$^{-/-}$ rMEFs. Thus the regulatory function of SHP on cyclin E gene transcription may be cell type–specific. Other studies have also pointed toward a role of SHP in cell cycle control, such as regulation of p21 promoter activity[25,26] and sexual maturation of male mice that involves several cyclins.[27] Thus, SHP may also play a role at different phases of cell cycle.

Loss of SHP function in *SHP*$^{-/-}$ mice enhanced hepatocyte proliferation and promoted transformation of hepatocytes. Consistent with this observation, the immortal *SHP* mutant MEFs showed enhanced proliferation and displayed characteristics of malignant transformed cells, including formation of more colonies in soft agar and promoting tumor growth in immune compromised mice. Based on observations from these two different cell types, we conclude that *SHP* deficiency is an important factor in promoting tumorigenesis.

It is noted that HCC was only developed in old *SHP*$^{-/-}$ mice. The transcriptional corepressor Tob gene has been identified as a tumor suppressor by repressing cyclin D1.[21] The mice lacking Tob did not show abnormalities in their early livers, but developed liver tumors by 18 months of age. Thus, the finding from both studies is very similar. Although the enhanced hepatocyte proliferation is directly associated with the development of HCC in *SHP*$^{-/-}$ mice, we consider it an initiating factor or first “hit.” A second hit, or other genetic alternations, may also be involved in HCC progression. For instance, bile acids have been shown to be promoting agents for HCC formation in nuclear receptor FXR knockout mice, which also showed increased cyclin D and cyclin E expression.[28] The levels of bile acids are also increased in *SHP*$^{-/-}$ livers due to loss of SHP repression of bile acid synthesis.[17] It is possible that bile acids may also promote the development of HCC in *SHP*$^{-/-}$ mice.

In conclusion, we show the novel effects of SHP on cellular proliferation and transformation. The future elucidation of how SHP modulates other signaling pathways, such as apoptosis signaling, will be of importance to our better understanding of nuclear receptors in the development of liver cancer.

Supplementary Material

Refer to Web version on PubMed Central for supplementary material.

Acknowledgments

The authors thank Dr. Curt Hagedorn for critical reading of the manuscript, Dr. Kazuhiro Oka for the adenoviruses, and Drs. Nan He and Jian-sheng Huang for their help.

Supported by funds from the American Liver Foundation/American Association for the Study of Liver Diseases (Liver Scholar Award), the American Diabetes Association (Junior Faculty Award), and the American Heart Association (BGIA Award) to L.W. and 2007AA02Z460 and 30370645.

NIH-PA Author Manuscript

NIH-PA Author Manuscript

NIH-PA Author Manuscript

Abbreviations

β-gal	β-galactosidase
BrdU	5-bromo-2'-deoxyuridine
CDK	cyclin-dependent kinase
FACS	fluorescence-activated cell sorting
FBS	fetal bovine serum
HCC	hepatocellular carcinoma
mCD1	mouse cyclin D1
MEF	mouse embryonic fibroblast
mRNA	messenger RNA
PCNA	proliferating cell nuclear antigen
SHP	small heterodimer partner

References

1. Sherr CJ. D-type cyclins. Trends Biochem Sci. 1995; 20:187–190. [PubMed: 7610482]
2. Harper JW, Elledge SJ. Cdk inhibitors in development and cancer. Curr Opin Genet Dev. 1996; 6:56–64. [PubMed: 8791491]
3. Bates SL, Bonetta L, Macallan D, Parry D, Holder A, Dickson C, et al. CDK6 (PLSTIRE) and CDK4 (PSKJ3) are a distinct subset of the cyclin-dependent kinases that associate with cyclin D1. Oncogene. 1994; 9:71–79. [PubMed: 8302605]
4. Mayol X, Garriga J, Grana X. Cell cycle-dependent phosphorylation of the retinoblastome-related protein p130. Oncogene. 1995; 11:801–808. [PubMed: 7651744]
5. Xiao ZX, Ginsberg D, Ewen M, Livingston DM. Regulation of the retinoblastoma protein-related protein p107 by G1 cyclin-associated kinases. Proc Natl Acad Sci U S A. 1996; 93:4633–4637. [PubMed: 8643455]
6. Hiebert SW, Chellappan SP, Horowitz JM, Nevins JR. The interaction of RB with E2F coincides with an inhibition of the transcriptional activity of E2F. Genes Dev. 1992; 6:177–185. [PubMed: 1531329]
7. Grana X, Reddy EP. Cell cycle control in mammalian cells: role of cyclins, cylin dependent kinases (CDKs), growth suppressor genes and cyclin-dependent kinase inhibitors (CKIs). Oncogene. 1995; 11:211–219. [PubMed: 7624138]
8. Dulic V, Lees E, Reed SI. Association of human cyclin E with a periodic G1-s phase protein kinase. Science. 1992; 257:1958–1961. [PubMed: 1329201]
9. Lundberg AS, Weinberg RA. Functional inactivation of the retinoblastoma protein requires sequential modification by at least two distince cyclin-cdk complexes. Mol Cell Biol. 1998; 18:753–761. [PubMed: 9447971]
10. Morgan DO. Cyclin-dependent kinases: engines, clocks, and microprocessors. Annu Rev Cell Dev Biol. 1997; 13:261–291. [PubMed: 9442875]
11. Diehl JA. Cyclin to cancer with cyclin D1. Cancer Biol Ther. 2002; 1:226–231. [PubMed: 12432268]
12. Sato Y, Itoh F, Hareyama M, Satoh M, Hinoda Y, Seto M, et al. Association of cyclin D1 expression with factors correlated with tumor progression in human hepatocellular carcinoma. J Gastroenterol. 1999; 34:486–493. [PubMed: 10452682]
13. Deane NG, Parker MA, Aramandla R, Diehl L, Lee WJ, Washington MK, et al. Hepatocellular carcinoma results from chronic cyclin D1 overexpression in transgenic mice. Cancer Res. 2001; 61:5389–5395. [PubMed: 11454681]

NIH-PA Author Manuscript

NIH-PA Author Manuscript

NIH-PA Author Manuscript

14. Bavner A, Sanyal S, Gustafsson JA, Treuter E. Transcriptional corepression by SHP: molecular mechanisms and physiological consequences. Trends Endocrinol Metab. 2005; 16:478–488. [PubMed: 16275121]
15. Wang L, Liu J, Saha P, Huang JS, Chan L, Spiegelman B, et al. The orphan nuclear receptor SHP regulates PGC-1 α expression and energy production in brown adipocytes. Cell Metab. 2005; 2:227–238. [PubMed: 16213225]
16. Wang L, Huang J, Saha P, Kulkarni RN, Hu M, Kim Y, et al. Orphan receptor small heterodimer partner is an important mediator of glucose homeostasis. Mol Endocrinol. 2006; 20:2671–2681. [PubMed: 16803864]
17. Wang L, Lee YK, Bundman D, Han Y, Thevananther S, Kim CS, et al. Redundant pathways for negative feedback regulation of bile acid production. Dev Cell. 2002; 2:721–731. [PubMed: 12062085]
18. Todaro GJ, Green H. Quantitative studies of the growth of mouse embryo cells in culture and their development into established lines. J Cell Biol. 1963; 17:299–313. [PubMed: 13985244]
19. Mateyak MK, Obaya AJ, Sedivy JM. c-Myc regulates cyclin D-Cdks and -Cdk6 activity but affects cell cycle progression at multiple independent points. Mol Cell Biol. 1999; 19:4672–4683. [PubMed: 10373516]
20. Tetsu O, McCormick F. Beta-catenin regulates expression of cyclin D1 in colon carcinoma cells. Nature. 1999; 398:422–426. [PubMed: 10201372]
21. Yoshida Y, Nakamura T, Komoda M, Satoh H, Suzuki T, Tsuzuku JK, et al. Mice lacking a transcriptional corepressor Tob are predisposed to cancer. Genes Dev. 2003; 17:1201–1206. [PubMed: 12756225]
22. Geng Y, Yu Q, Sicinska E, Das M, Schneider JE, Bhattacharya S, et al. Cyclin E ablation in the mouse. Cell. 2003; 114:431–443. [PubMed: 12941272]
23. Ortega S, Prieto I, Odajima J, Martin A, Dubus P, Sotillo R, et al. Cyclin-dependent kinase 2 is essential for meiosis but not for mitotic cell division in mice. Nat Genet. 2003; 35:25–31. [PubMed: 12923533]
24. Botrugno OA, Fayard E, Annicotte JS, Haby C, Brennan T, Wendling O, et al. Synergy between LRH-1 and beta-catenin induces G1 cyclin-mediated cell proliferation. Mol Cell. 2004; 15:499–509. [PubMed: 15327767]
25. Kim JY, Chu K, Kim HJ, Seong HA, Park KC, Sanyal S, et al. Orphan nuclear receptor small heterodimer partner, a novel corepressor for a basic helix-loop-helix transcription factor BETA2/neuroD. Mol Endocrinol. 2004; 18:776–790. [PubMed: 14752053]
26. Suh JH, Huang J, Park YY, Seong HA, Kim D, Shong M, et al. Orphan nuclear receptor small heterodimer partner inhibits transforming growth factor-beta signaling by repressing SMAD3 transactivation. J Biol Chem. 2006; 281:39169–39178. [PubMed: 17074765]
27. Volle DH, Duggavathi R, Magnier BC, Houten SM, Cummins CL, Lobaccaro JM, et al. The small heterodimer partner is a gonadal gatekeeper of sexual maturation in male mice. Genes Dev. 2007; 21:303–315. [PubMed: 17289919]
28. Yang F, Huang X, Yi T, Yen Y, Moore DD, Huang W. Spontaneous development of liver tumors in the absence of the bile acid receptor farnesoid X receptor. Cancer Res. 2007; 67:863–867. [PubMed: 17283114]

NIH-PA Author Manuscript
NIH-PA Author Manuscript
NIH-PA Author Manuscript

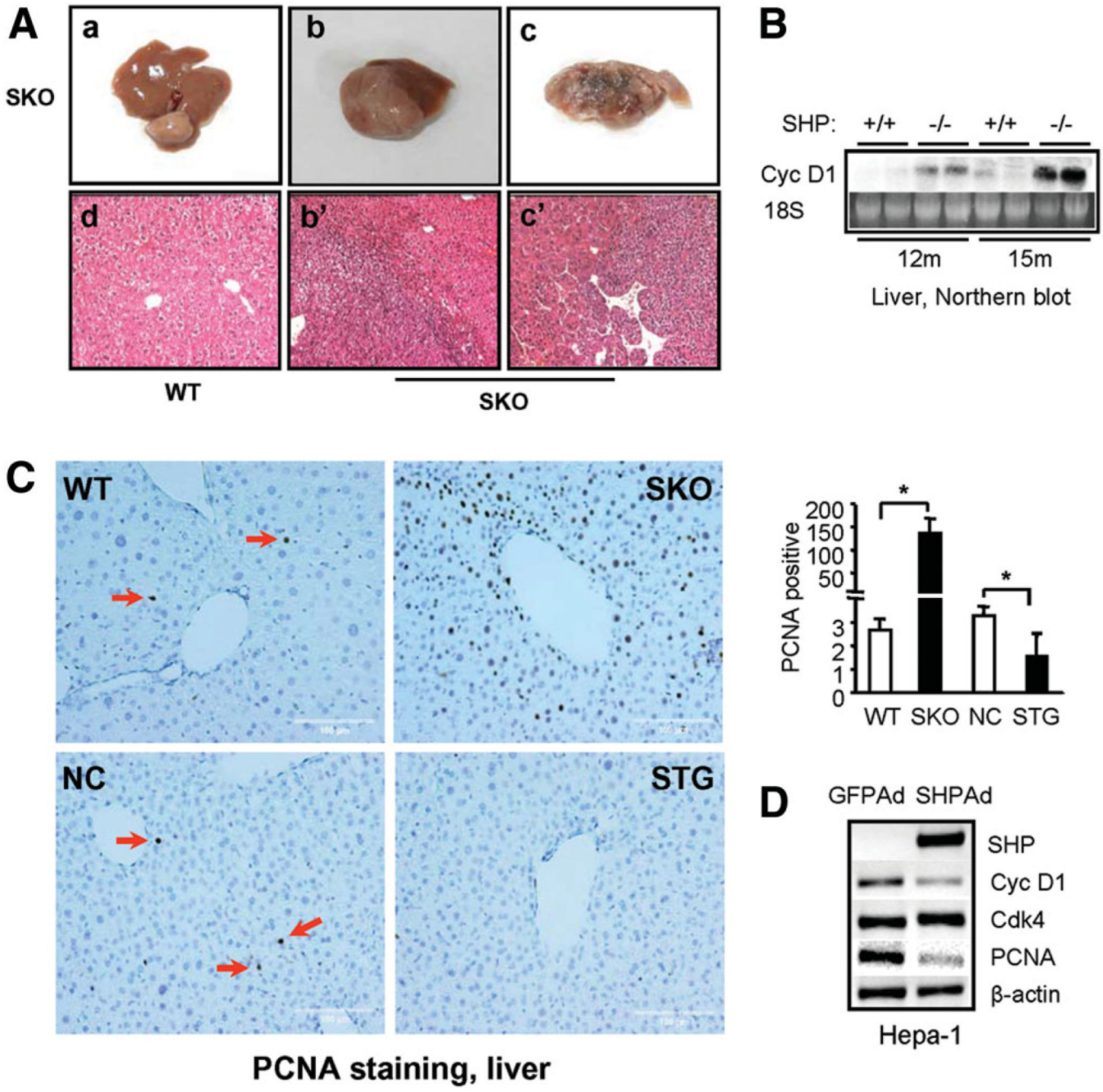

Fig. 1.

Spontaneous formation of HCC in mice lacking *SHP*. (A) *SHP*$^{-/-}$ mice developed HCC at 15 months of age (panels a-c). Hema-toxylin-eosin staining of wild-type (WT) liver (panel d) and tumors b and c (panels b' and c'). (B) Increased cyclin D1 expression in *SHP*$^{-/-}$ liver compared with wild-type mice by northern blotting. (C) Massive hepatocyte proliferation in livers of *SHP*$^{-/-}$ (SKO) mice, which was inhibited in *SHP*-transgenic (STG) mice. NC, nontransgene controls. Ten- to 12-month-old mice were used for the assay. Bar graph represents mean ± SD of PCNA-positive cells counted in three fields per slide (n = 3). (D) SHP inhibition of cyclin D1 and PCNA expression in mouse HCC cell line Hepa-1 cells as examined by semiquantitative polymerase chain reaction analysis.

NIH-PA Author Manuscript
NIH-PA Author Manuscript
NIH-PA Author Manuscript

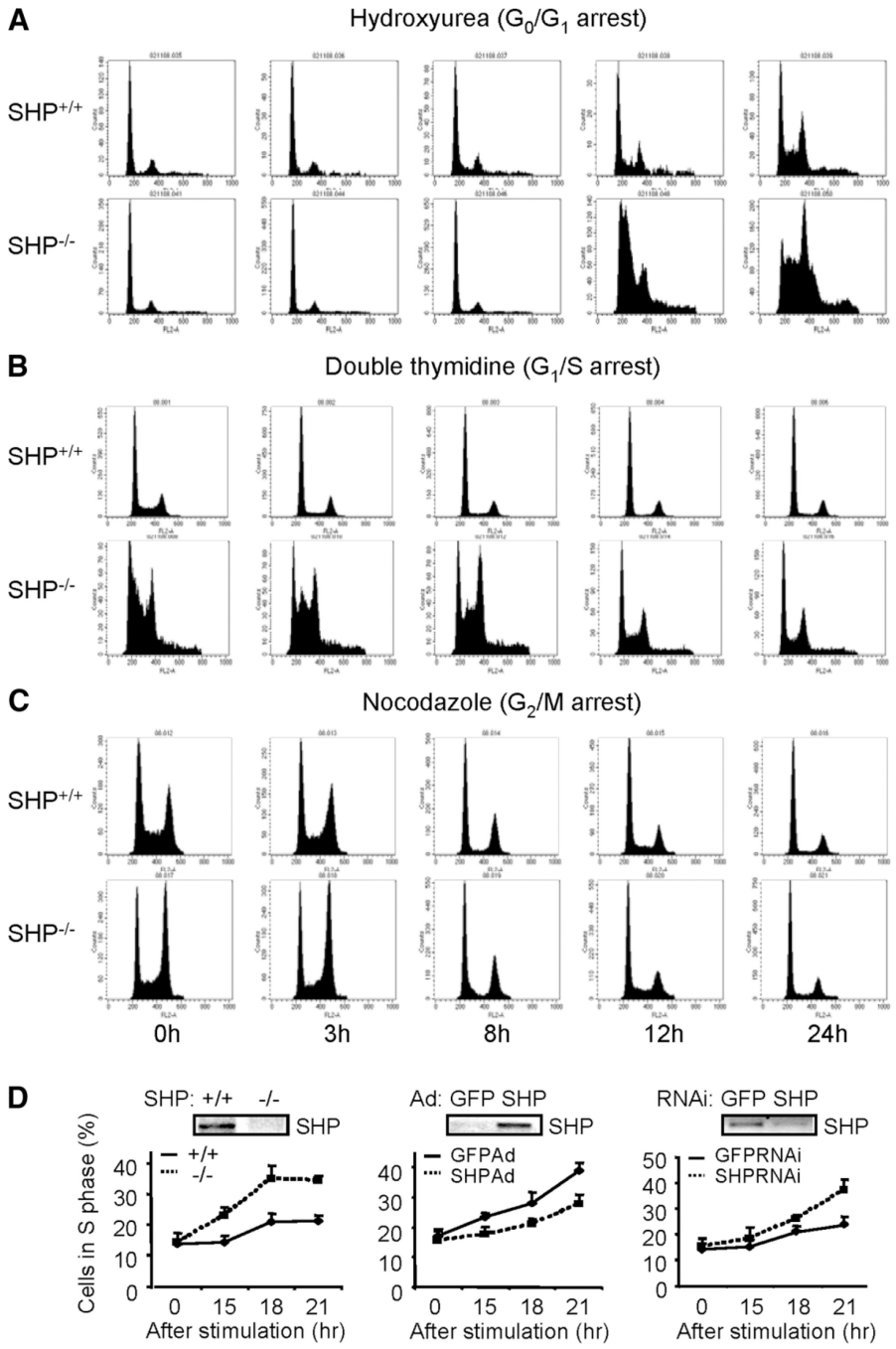

Fig. 2.

Enhanced proliferation of immortalized fibroblasts lacking *SHP*. (A) FACS analysis of $SHP^{+/+}$ and $SHP^{-/-}$MEFs synchronized at G_0/G_1 by hydroxyurea. (B) FACS analysis of $SHP^{+/+}$ and $SHP^{-/-}$ MEFs synchronized at G_1/S by double thymidine block. (C) FACS analysis of $SHP^{+/+}$ and $SHP^{-/-}$ MEFs arrested at G_2/M phase by nocodazole. (D) FACS analysis of cells synchronized at G_0 by serum starvation and released into the cell cycle. Left: $SHP^{+/+}$ and $SHP^{-/-}$ cells in S phase; middle: re-expressing SHP in $SHP^{-/-}$ cells by adenovirus; right: knocking down SHP in $SHP^{+/+}$ cells by RNA interference. GFP, control virus.

NIH-PA Author Manuscript
NIH-PA Author Manuscript
NIH-PA Author Manuscript

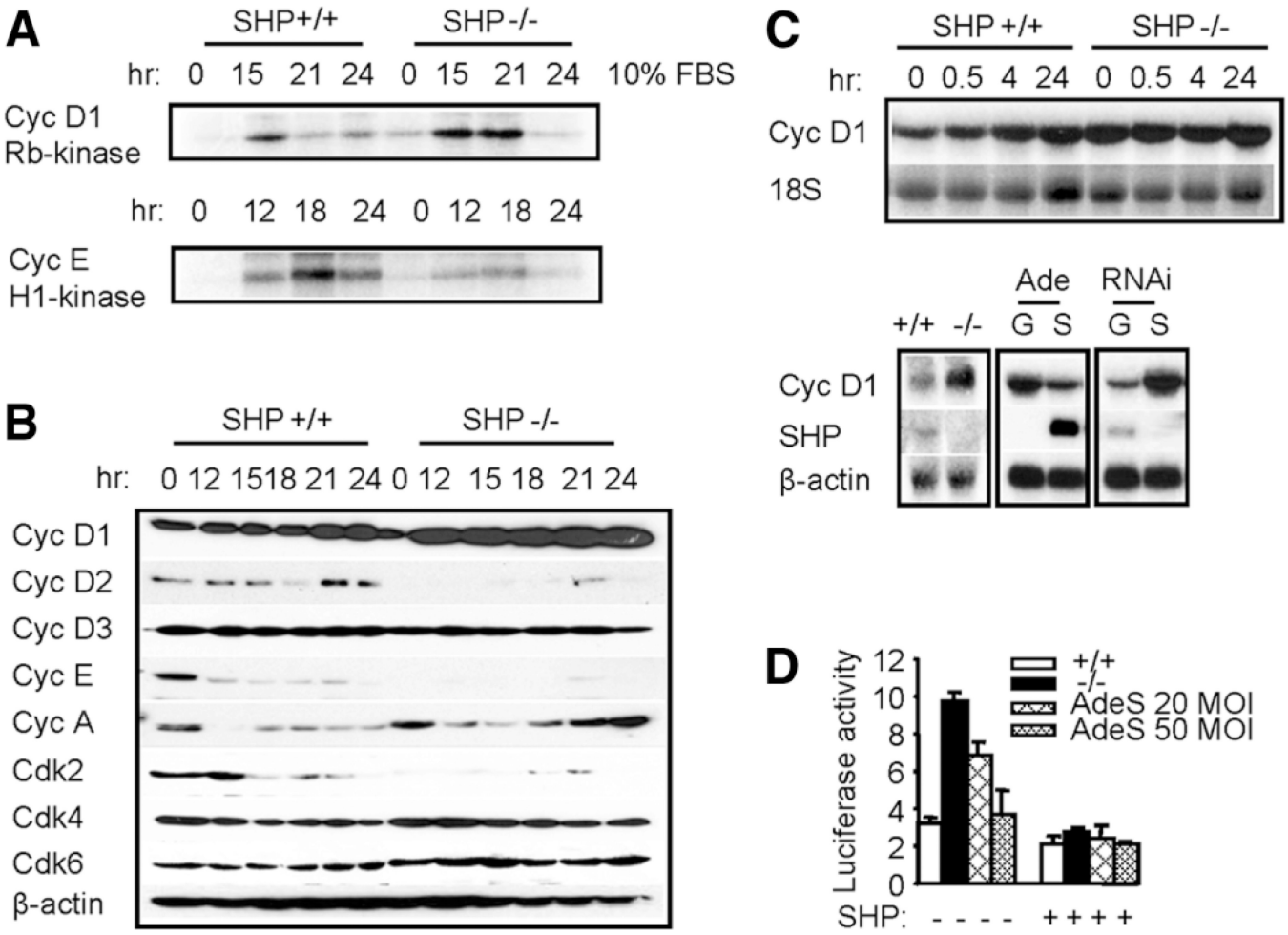

Fig. 3.

Changes of cyclins and CDKs lacking *SHP* and inhibition of cyclin D1 mRNA by SHP. (A) Changes of cyclin D1/pRb-kinase activity and cyclin E/H1-kinase activity in $SHP^{+/+}$ and $SHP^{-/-}$ fibroblasts. Cyclin D-associated or cyclin E-associated protein complexes were immunoprecipitated from cell lysates, and GST-Rb or histone H1 kinase activity was measured as described in Materials and Methods. (B) Expression of cell cycle regulatory proteins via western blotting in synchronized and restimulated $SHP^{+/+}$ and $SHP^{-/-}$ fibroblasts. (C) Top: expression of cyclin D1 mRNA in synchronized and restimulated fibroblasts as determined by northern blot. Bottom: expression of cyclin D1 mRNA was increased in exponential growing $SHP^{-/-}$ cells (left), decreased by overexpressing SHP (middle), and increased by knocking down *SHP* function (right), as determined via northern blotting. G, green fluorescent protein; S, SHP. (D) Cyclin D1 promoter activity. Both the $SHP^{+/+}$ and $SHP^{-/-}$ cells were transfected with a mouse cyclin D1 promoter reporter with or without SHP expression vector, and promoter activity was measured via luciferase/β-gal assay. AdeS, adenovirus SHP.

NIH-PA Author Manuscript
NIH-PA Author Manuscript
NIH-PA Author Manuscript

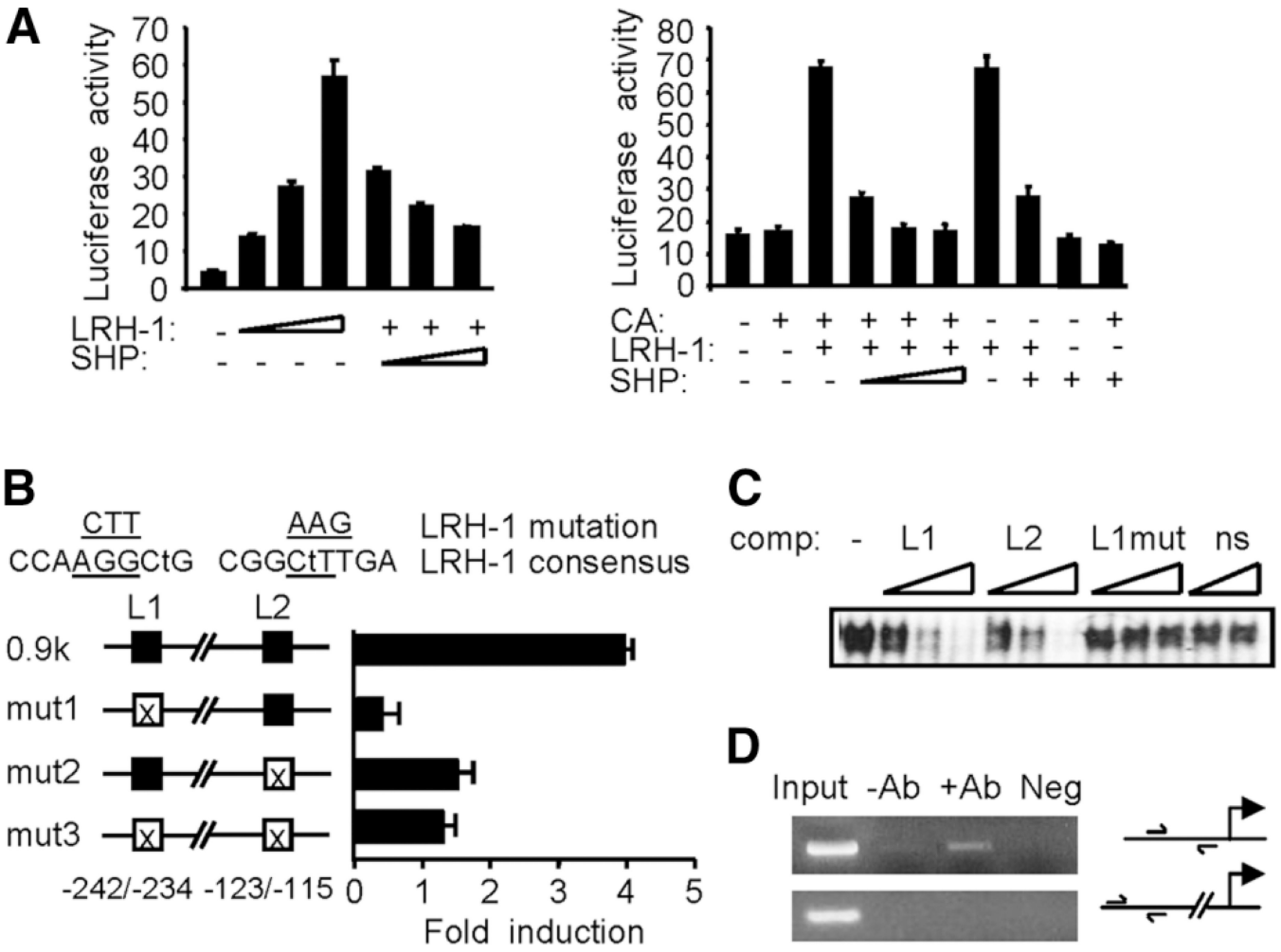

Fig. 4.

Transcriptional repression of cyclin D1 promoter by SHP. (A) Left: a − 187mCD1-Luc was transfected into CV-1 cells with LRH-1 (50, 100, 200 ng) in the absence (−) or presence (+) of SHP (100, 200, 300 ng). Right: reporter gene of −970mCD1-Luc was cotransfected with expression vectors for β-catenin (CA, 400 ng), LRH-1 (100 ng), and SHP (100, 200, 300 ng; fixed amount: 200 ng) as indicated. Luciferase activities were normalized against β-galactosidase and expressed as relative activity. (B) Mutagenesis study. The mCD1 gene contains two potential LRH-1 sites (L1, L2). Mismatches with the consensus sequence are indicated by lower case letters, and mutated sequences are underlined. The mutated constructs (mut1, mut2, and mut3) were transfected into CV-1 cells with or without LRH-1 (100 ng). (C) Gel shift assay. *In vitro* translated LRH-1 was incubated with the ^{32}P-labeled L1 and increasing amounts of unlabeled L1 (lanes 2–4), L2 (lanes 5–7), and mutated L1 (lanes 8–10) or HNF-4 binding sequences (ns: lanes 11–12). (D) Chromatin immunoprecipitation analysis. Chromatin preparations from MEFs were subjected to chromatin immunoprecipitation assay with anti-SHP antibodies. DNA in the immunoprecipitates was polymerase chain reaction-amplified with the primers shown in the illustration of the promoter region. DNA from equal amounts of chromatin was polymerase chain reaction amplified before immunoprecipitation (Input). Neg, immunoglobulin G.

NIH-PA Author Manuscript

NIH-PA Author Manuscript

NIH-PA Author Manuscript

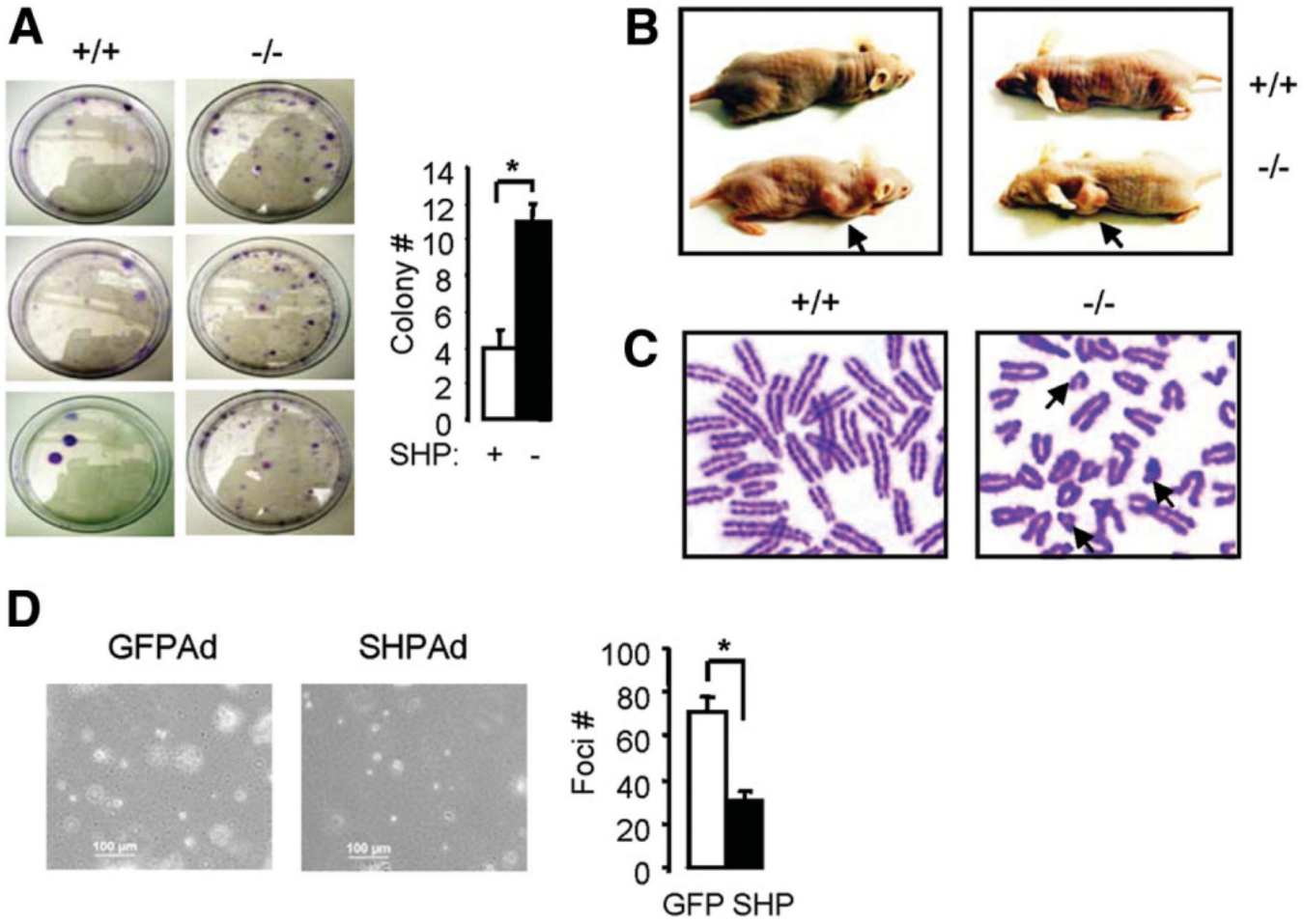

Fig. 5.

Transformation and tumorigenesis of immortalized fibroblasts lacking *SHP*. (A) Colony formation assay. Results from three independent $SHP^{+/+}$ and $SHP^{-/-}$ cells were shown. (B) Tumorigenicity assay in nude mice. Four wild-type and five *SHP* mutant 3T3 clones were tested. Nude mice were still tumor-free 6 weeks after injection of wild-type MEF cells, whereas tumors (arrows) were observed 4 weeks after injection of $SHP^{-/-}$ cells. Photographs were taken 6 weeks after injection. (C) Chromosome spreads of $SHP^{+/+}$ and $SHP^{-/-}$ 3T3 cells to examine chromosome aberrations. Each metaphase spread was assessed for the frequency of chromosome abnormalities. Note that only parts of spreads are shown in order to highlight the short chromosomes (arrows) found in $SHP^{-/-}$ cells. (D) Foci formation assay. SHP was overexpressed into $SHP^{-/-}$ fibroblasts by adenovirus transduction. Statistical results represent the mean ± standard deviation of foci counts from two different fields of triplicate plates.